Development of Low Cost MAGLEV Vehicle for Semiconductor Transport System

No. 54

So-Young Sung, Je-Sung Bang, Ho-Kyung Sung, Han-Wook Cho
System Engineering Research Division, Korea Institute of Machinery and Materials, Daejeon, Korea
takladst@yahoo.co.kr, hwcho@kimm.re.kr, sung-hk@kimm.re.kr, jsbang@kimm.re.kr

Jang-Young Choi, Seok-Myeong Jang
Department of Electrical Engineering, Chungnam National University, Daejeon, Korea
aramis76@cnu.ac.kr, smjang@cnu.ac.kr

ABSTRACT: This paper deals with a design process of electromagnet for MAGLEV Vehicle for Semiconductor Transport (STMAG) and proposes a nonlinear suspension model for accurate levitation control. Their sensor's bandwidth can be deduced to build a sensor. Comparing control gain in simulating non-linear model to real experiments, and confirming that the gain is similar, we confirm that the nonlinear suspension model is superior to linear model. Also, in order to guarantee 365 days/24 hours operating condition, the influence of the winding temperature on the levitation control is also investigated. Finally, the validity of design process and non-linear model for levitation control proposed in this paper are described.

1 INTRODUCTION

Since Hermann Kemper in Germany proposed magnetic suspension system in 1934, the system has been developed in many fields thanks to considerable technological improvement in 1960s[1]. Electromagnetic suspension system can be divided into Electrodynamics Suspension system (EDS), Electromagnet Suspension system (EMS), and most recent hybrid forms using permanent magnet. Applications of magnetic suspension systems with its possibility of replacing wheel-type railroad systems, have been developed into Transrapid in Germany[2], HSST[3] and MLX[4] in Japan and UTM[5] in Korea. Another important application of EMS system is the transport system in semiconductor manufacturing line, of which further studies have not made much development, despite of the general interest in this system. The EMS system in semiconductor manufacturing line requires higher reliability, since it needs to run 365 days 24 hours in same conditions. To use EMS system in manufacturing line for transportation system, the price of whole system should be lower, at least similar to previous proposed or implemented systems. However, previously proposed EMS system used high cost sensor and control systems, which made EMS systems hard to compete with other transportation systems in price.

This paper discusses the development of a low cost MAGLEV Vehicle for Semiconductor Transport (STMAG). We designed and manufactured the acceleration sensor using *i*MEMS type sensor. We use the low cost proximity type sensor. In addition, we designed and manufactured the electromagnet (EM) using commercial square-type copper coil instead of special order made aluminum sheet coil. For computation of suspension control algorithm, TI's TMS320F28335 as Floating Point DSP is used for suspension control. The nonlinear suspension system is modeled to suspect more accurate control gain than linear model. To guarantee 365 days/24 hours operating condition, it needs to design to reduce the parameter variation. The current density of EM is limited to 2[A/mm] to minimize the temperature variation, so that the increase of the EM temperature can not be over 20 degrees. The power supply system for STMAG is adopted Non-Contact Power (NCP) supply.

2 TECHNOLOGY DEVELOPMENT

2.1 Design of Suspension Electromagnets

The required specification and design constraints of EM for STMAG are shown in table 1. The stored energy and inductance of EM are given by eq. (1), (2). From eq. (1), the levitation force given by eq. (3).

$$w_m(t) = \frac{1}{2} L(i,z,t) i^2(t) \tag{1}$$

$$L(i,z,t) = N\frac{\psi(t)}{i(t)} = \frac{N}{i(t)}\frac{Ni(t)}{R_m} = \frac{\mu_0 N^2 a_m}{2z(t)} \tag{2}$$

$$\begin{aligned} F(z,i,t) &= \frac{dw_m(t)}{dt} = \frac{d}{dz}\left[\frac{1}{2}L(z,i,t)i^2(t)\right] \\ &= \frac{\mu_0 N^2 a_m}{4}\left[\frac{i(t)}{z(t)}\right]^2 \end{aligned} \tag{3}$$

Where, $\psi(t)$, N, a_m, $z(t)$, R_m, μ_0 are air-gap flux, number of winding, sectional area of EM, reluctance and permeability of air gap, respectively.

Table 1 Required specification and design constraints of EM.

Required Sepcification			
Levitation Force	1000[N]	Nominal air-gap	3[mm]
		Nominal current	< 5[A]
Design constraints			
Magnet depth (w)	≤ 200[mm]	Magnet width (l+2d)	≤160[mm]
Magnet height (h)	≤ 50[mm]		

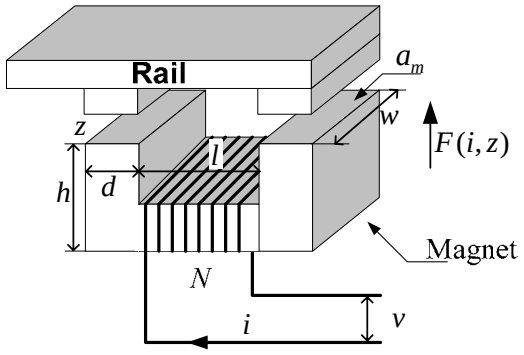

Figure 1 Electromagnet suspension system.

According to the required specification and design constraint in table 1, pole length d in figure 1 is adjusted. After winding area lw and sectional area dw is calculated, winding number according to the rate current of coil diameter can be yielded. The calculated winding number, rate current of coil diameter and pole area are used to calculate levitation force. The process of yielding d and l in maximum levitation force is shown in figure 2.

2.2 Nonlinear model of EMS system and controller design

The Voltage and dynamic equation of EMS system likely figure 1 can be expressed as eq. (4). Choosing state variable $x(t) = [\dot{z}(t), \ddot{z}(t), i(t)]^T$ in eq. (3), nonlinear state equation can be expressed as eq. (4). In eq. (4) v is supply voltage of EM. Generally, eq. (4) is linearized in nominal point (i_0, z_0) to analyze stability of EMS system. However, we designed nonlinear modeling for EMS system from eq. (4) and (5) using Matlab/Simulink. The related block diagram of nonlinear model is shown in figure 3.

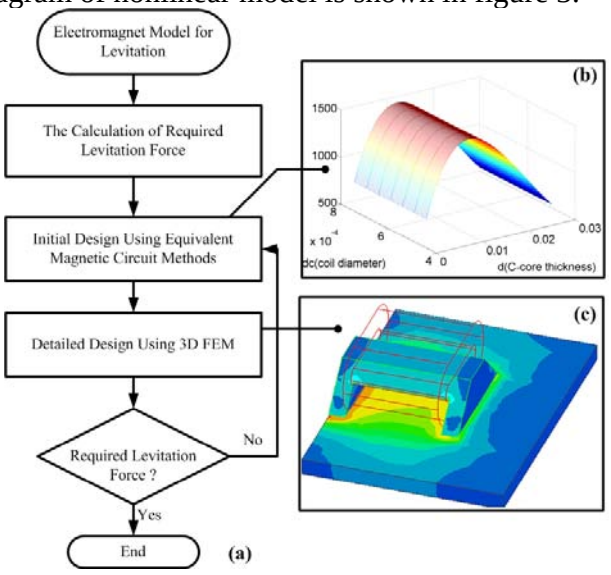

Figure 2 Electromagnet Design: (a) Design Process, (b) Initial design Result (c) 3D FEM Analysis.

$$\begin{aligned} m\frac{d^2z(t)}{dt^2} &= -F(i,z,t) + f_d + mg \\ &= -\frac{\mu_0 N^2 a_m}{4}\left(\frac{z(t)}{i(t)}\right)^2 + f_d + mg \\ \frac{di(t)}{dt} &= \frac{i(t)}{z(t)}\frac{dz(t)}{dt} \\ &\quad -\frac{2}{\mu_0 N^2 a_m} z(t)(R_m i(t) - v(t)) \end{aligned} \tag{4}$$

$$\begin{aligned} \dot{x}_1 &= x_2 \\ \dot{x}_2 &= -\frac{\mu_0 N^2 a_m}{4m}\left(\frac{x_3}{x_1}\right)^2 + g + \frac{f_d}{m} \\ \dot{x}_3 &= \frac{x_3}{x_1}x_2 - \frac{2R_m}{\mu_0 N^2 a_m}x_1 x_3 + \frac{2x_1}{\mu_o N^2 a_m}v \\ y &= x_1 \end{aligned} \tag{5}$$

From figure 1, the reluctance can be expressed as eq. (6) and flux, flux linkage, inductance and flux density can be expressed as eq. (7)

$$R_g(t)=\frac{z(t)}{\mu_0 a_m} \tag{6}$$

$$\begin{aligned}\psi(t)&=\frac{Ni(t)}{2R_g}=\frac{Ni(t)}{2}\frac{\mu_0 a_m}{z(t)},\\ \lambda(t)&=N\psi(t)=\frac{N^2 i(t)}{2}\frac{\mu_0 a_m}{z(t)},\\ L(t)&=\frac{\lambda(t)}{i(t)}=\frac{\mu_0 N^2 a_m}{2z(t)},\\ B(t)&=\frac{\psi(t)}{a_m}=\frac{\mu_0 Ni(t)}{2z(t)}.\end{aligned} \tag{7}$$

Since having inherited open loop instability, the EMS control system requires feedback control. Generally state feedback controller is adopted and its control law can be expressed as eq. (8). Where, k_p, k_v, k_a, $z_{ref}(t)$, $a(t)$ is proportional, velocity, acceleration gain, reference air-gap and acceleration signal from dynamic filter output, respectively.

$$u(t)=v(t)=k_p(x_1(t)-z_{ref})+k_v x_2(t)+k_a a(t) \tag{8}$$

To apply state feedback controller, it needs to measure state variable of eq. (5), but it is impossible to measure velocity signal directly. Hence, it is necessary to develop an algorithm which can estimate velocity from acceleration and air gap sensor. We used the dynamic filter applied in UTM in Korea to measure velocity. Eq. (9) shows state matrixes of dynamic filter[5]. The frequency response of dynamic filter and system simulation results of nonlinear EMS model are shown in figure 4 and 5, respectively.

$$\begin{aligned}A_{df}&=\begin{bmatrix}-6.403 & 5929 & -3.198 & -6.259e\text{-}12 & 1.425\\ -3.952e\text{-}19 & -910.9 & 5.588e\text{-}15 & -5.111e\text{-}15 & -50.16\\ 5 & -4558 & 0.001998 & 9.135e\text{-}13 & -1.083\\ 5.002 & -1.349 & 9.492e\text{-}06 & -100 & 49.93\\ 0 & 4559 & -2.813e\text{-}14 & 2.011e\text{-}14 & 0.9082\end{bmatrix},\\ B_{df}&=\begin{bmatrix}4e+06 & -1.136e+05\\ 4.827e\text{-}15 & 4.013e+06\\ -0.6668 & 8.619e+04\\ -11.9 & 5381\\ -2.518e\text{-}15 & -8.6e+04\end{bmatrix}, D_{df}=\begin{bmatrix}0 & 0.003179\\ 0 & 0.5086\\ 7.71e\text{-}06 & 4.434e\text{-}05\\ 0.0006245 & 0.000413\\ 0.9992 & 0.6608\end{bmatrix},\\ C_{df}&=\begin{bmatrix}0 & 6.357e\text{-}6 & 0 & 0 & 1.246e\text{-}5\\ 0 & 0.001017 & 0 & 0 & -6.357e\text{-}6\\ 1.542e\text{-}8 & 8.868e\text{-}8 & -6.164e\text{-}12 & 2.469e\text{-}5 & 1.538e\text{-}7\\ 1.249e\text{-}6 & 8.26e\text{-}7 & -4.993e\text{-}10 & 0 & -5.163e\text{-}9\\ -1.624e\text{-}6 & 0.001322 & -7.988e\text{-}7 & 0 & -8.26e\text{-}6\end{bmatrix}.\end{aligned} \tag{9}$$

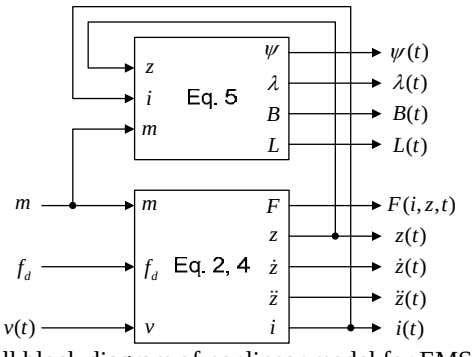

(a) Overall block diagram of nonlinear model for EMS system.

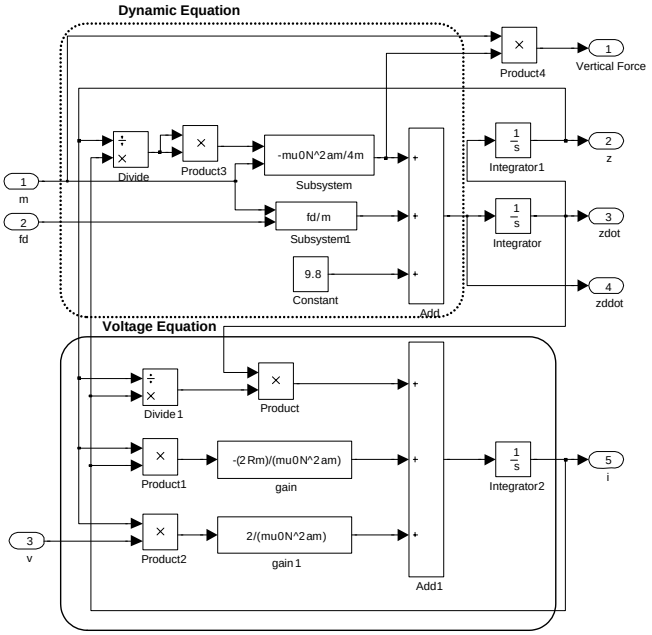

(b) Electro-mechanical subsystem of EMS system.

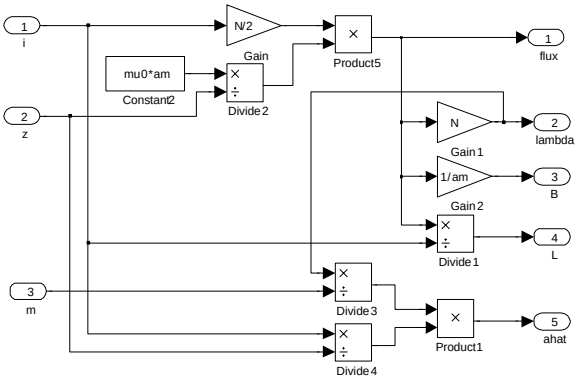

(c) Electro-Magnetic subsystem of EMS System.

Figure 3 Nonlinear model of EMS system.

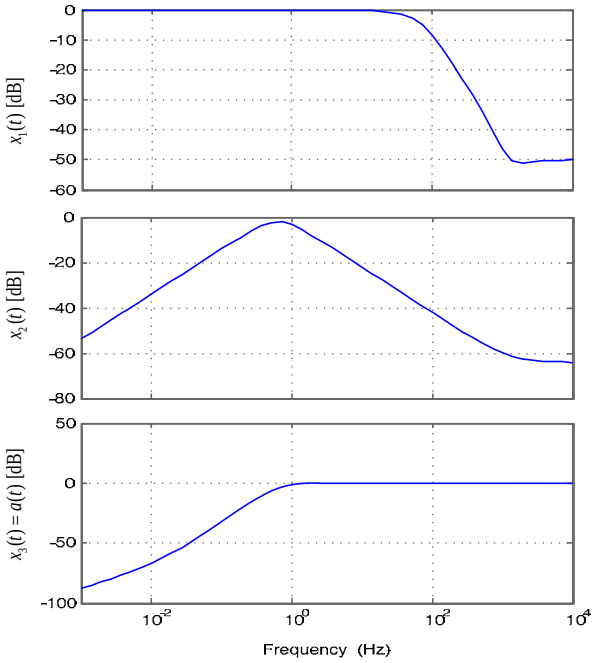

Figure 4 Frequency response of dynamic filter

2.3 *Sensor System and Stability analysis*

In linear system, it is possible to analyze the stability of the system with linear algebra. However, in nonlinear system, it is necessary to confirm that Phase Trajectory of state variables converges to a nominal point. In implemented system, low pass filter is commonly used to remove noise from sensors,. To define bandwidth of low pass filter, a system shown in figure 6 is constructed to compare cut off frequency of sensor input. The results are shown in figure 7. We adopted the second order Butter-worth filter as low pass filter.

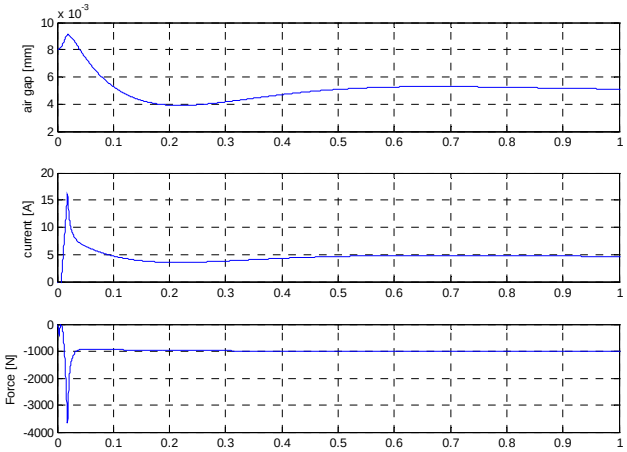

(a) Dynamic simulation of Electro-Mechanical subsystem.

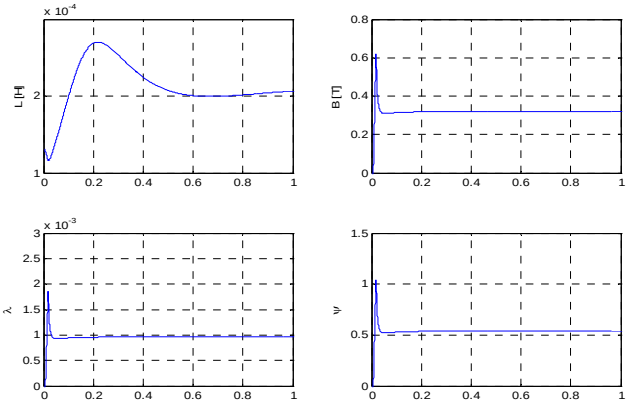

(b) Dynamic simulation of Electro-Magnetic subsystem.

Figure 5 Results of dynamic simulation.

As shown in figure 7, the system stability can be achieved when the bandwidth of filter is over 500Hz. The system sensitivity is affected by acceleration sensor than air gap sensor. We designed and manufactured acceleration sensor using ADXL321 of Analog device Co. Ltd., the sensor has maximum $\pm 18g$ range. For dynamic range control, the designed sensor has two ranges; $\pm 1g$, $\pm 10g$, respectively. The designed acceleration sensor and proximity type air-gap sensor are shown in figure 8.

The air gap sensor has nonlinear characteristics against air-gap. Therefore the sensors are calibrated and we are find curve fit function of 3rd order polynomial to suspension control. The air-gap sensor response and curve fit function are shown in figure 9.

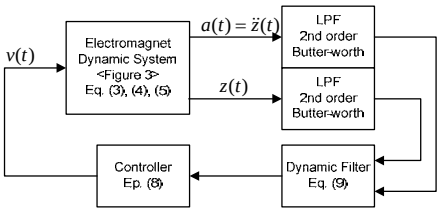

Figure 6 Overall block diagram for dynamic simulation.

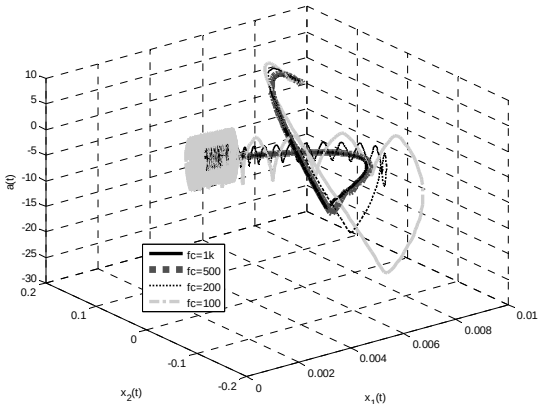

Figure 7 Phase trajectory of EMS system.

Figure 8 A designed acceleration sensor and air-gap sensor.

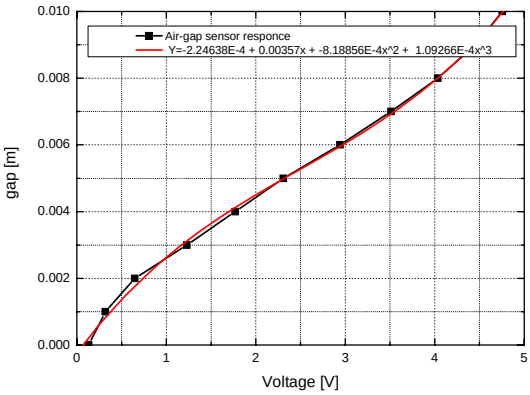

Figure 9 Air-gap sensor response and 3rd order curve fit function.

2.4 *Experimental Setup and Results*

We design and manufactured a controlling system; General Purpose High Speed Real Time Control System (GPHSRT-CS) using TMS320F28335 TI's Floating Point DSP. The GPHSRT-CS has two CPU boards, two 8CH isolated analog interface board, a

digital input-output board which has 32 Channels. The CPU board has maximum 16 CH analog input, 8CH PWM Ports, 8CH analog output, 2CH SCI and 1CH encoder input. The GPHSRT-CS system is shown in figure 10. The whole transportation system block diagram is shown in figure 11. The power supply system for STMAG is adapted Non-Contact Power (NCP) supply manufactured by Woosung Mechatronics Co. Ltd. in Korea. The NCP has primary power transfer system and secondary pickup system. One is full bridge power electronics circuit that is driven by 20[kHz] sine wave type power line. The other component is power collector with ferrite core inductor. The regulator is located at STMAG. It rectifies the high frequency AC power to 300VDC. Also, the DC/DC converter for chopper is installed at STMAG. It converts the DCLINK voltage from 300VDC to 100VDC. The chopper is half-bridge power electronics circuit with Intelligent Power Module (IPM). The propulsion system employed the Linear Induction Motor (LIM) drives with the VVVF Inverter. The rated current and velocity of LIM are 5[A] and 5[m/s], respectively. The manufactured STMAG and NCP are shown in figure 12 and detailed explanation about sub-components is listed in table 2 and figure 13. The experimental results of STMAG system are shown in figure 14 and 15.

Figure 10 Designed GPHSRT-CS system.

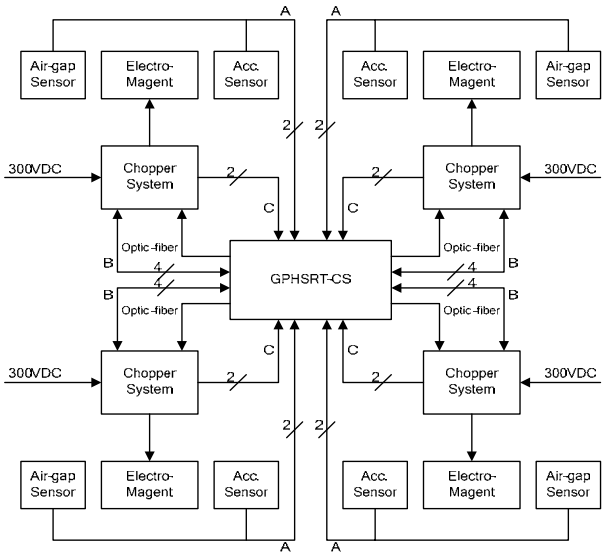

Figure 11 Block diagram of whole system for STMAG.

Figure 12 Pictures of STMAG and Non-Contact Power supply.

Table 2 Sub-components of STMAG

No	Name	Quantity
①	2nd suspension	4
②	Linear Induction motor	2
③	Acceleration sensor	4
④	Levitation magnet	4
⑤	Non-contact power supply	1
⑥	Vertical landing gear	4
⑦	Side landing gear	4
⑧	Gap sensor	8
⑨	Steel guide way	1
⑩	Aluminum conduct plate	2

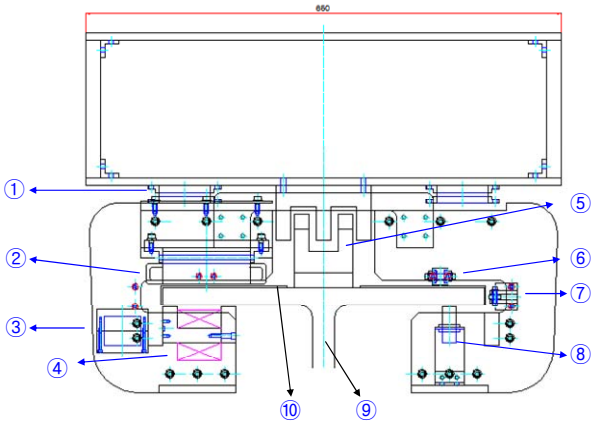

(a) Front view

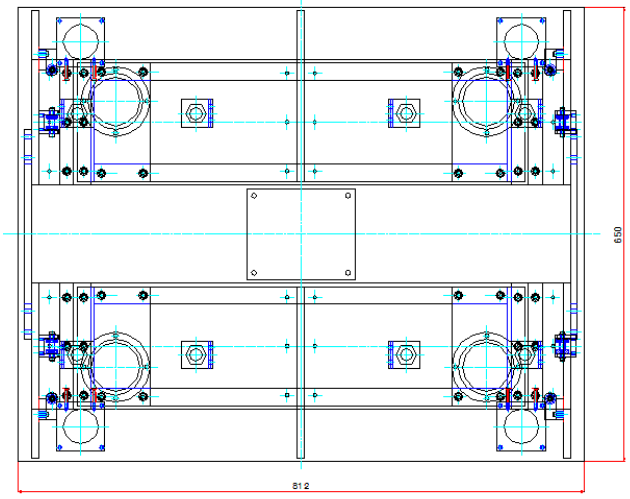

(b) Top View

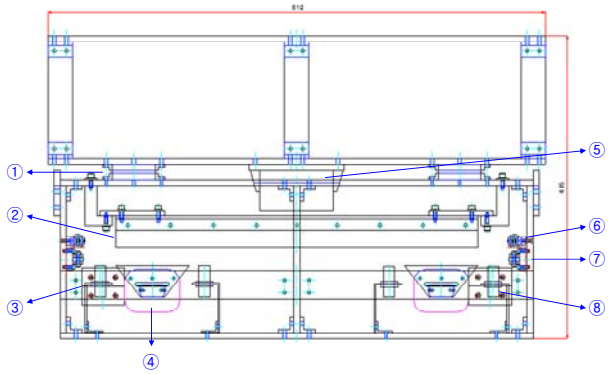

(c) Side view

Figure 13 Sub-component of STMAG

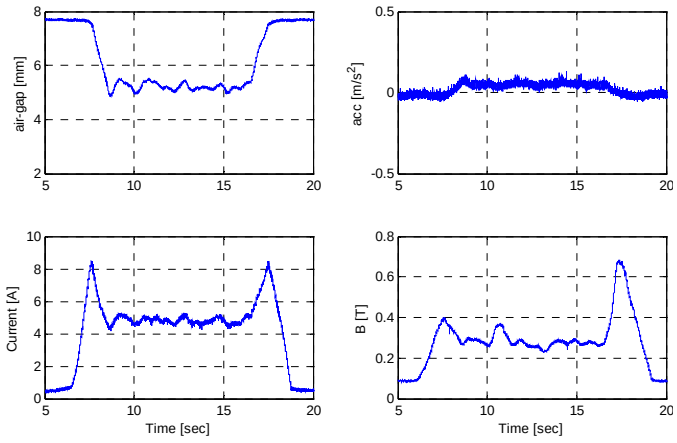

Figure 14 Experimental Results of STMAG

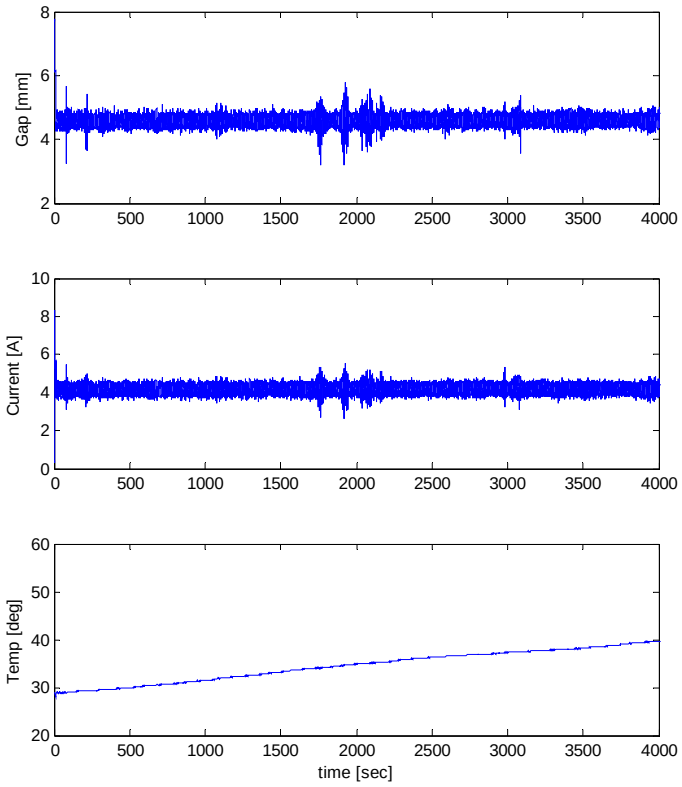

Figure 15 Experiment Results of long time operation.

3 CONCLUSIONS

This paper has defined a design process of electromagnet for STMAG, proposed a nonlinear suspension model, of which sensor's bandwidth can be deduced to build a sensor. Comparing control gain in simulating non-linear model to real experiments, and confirming that the gain is similar, we have verified the superiority of the nonlinear suspension model to linear model. To guarantee 365 days/24 hours operating condition, this paper has also confirmed that the increase of the EM temperature is not over 20 degrees. As a consequence, the validity of design process and non-linear model for levitation control proposed in this paper has been verified.

4 REFERENCES

[1] Hyung-Woo Lee, Ki-Chan Kim and Ju Lee, "Review of Maglev Train Technologies", IEEE Trans. on Magnetics, Vol. 42, No,7 July 2006

[2] Meins, J.; Miller, L.; Mayer, W.J., "The high speed Maglev transport system TRANSRAPID" Magnetics, IEEE Transactions on Volume 24, Issue 2, Part 2, Mar 1988

[3] Nakamura, S., "Development of high speed surface transport system (IISST)", Magnetics, IEEE Transactions on Volume 15, Issue 6, Nov 1979

[4] Cassat, A.; Jufer, M., "MAGLEV projects technology aspects and choices", Applied Superconductivity, IEEE Transactions on Volume 12, Issue 1, March 2002

[5] H.K. Sung, S.H. Lee and Z. Bien, "Design and implementation of a fault tolerant controller for EMS systems", Mechatronics Volume 15, Issue 10, December 2005